Rodriguésia 71: e01662018. 2020
http://rodriguesia.jbrj.gov.br
DOI: http://dx.doi.org/10.1590/2175-7860202071024

Original Paper

An inexpensive and environmentally friendly staining method for semi-permanent slides from plant material probed using anatomical and computational chemistry analyses

Cleber José da Silva[1,3,4], *Leonardo Henrique França de Lima*[2], *Priscila Marques de Paiva*[1], *Luana Malaquias Maia*[1], *Rafael Eduardo de Oliveira Rocha*[2], *Pedro Thiago Duarte de Souza*[2], & *Deise Aparecida de Castro Araújo Carvalho*[1]

Abstract

One of the main methods for plant anatomy study is the analysis of thin, transparent, and stained tissue sections. Synthetic dyes traditionally used in anatomical studies might be expensive and produced by specific companies. In contrast, the use of alternative industrial dyes can both represent an inexpensive substitute as well as an environmentally friendly option for conducting plant anatomy studies. In this study, a set of 22 textile dyes was evaluated. Transversal-, longitudinal, and paradermal sections of plant organs obtained using the freehand cutting technique were stained using hydroalcoholic solution (0 to 100%) of textile dyes purchased from a local market. Dyes mixed with 50% hydroalcoholic solution showed higher efficiency in tissue contrast, allowing greater solubility of dye powder and better solution interaction with the plant tissues. Most of the tested dyes showed satisfactory staining results. Cell wall, especially lignified one, showed higher staining efficiency. Computational docking analysis and molecular models of cellulose and lignin showed the probable association mechanisms and dye selectivity to cell wall constituents. Our findings suggest that the developed method can be useful in mixed practical classes of plant anatomy, chemistry, and/or biochemistry, both at high school as well as undergraduate levels.

Key words: computational chemistry, inexpensive methodology, plant anatomy, staining method, textile dyes.

Resumo

Um dos principais métodos para estudo de anatomia das plantas é a análise de cortes finos e transparentes, submetidos à coloração. Corantes sintéticos tradicionalmente utilizados em estudos anatômicos podem ser caros e produzidos por empresas específicas. O uso alternativo de corantes têxteis industriais, pode representar tanto uma substituição acessível economicamente quanto uma opção ecologicamente viável de uso desses corantes. Neste estudo foram avaliados 22 tipos de corantes têxteis. Cortes transversais, longitudinais e paradérmicos de órgãos de plantas, obtidos pela técnica de corte à mão livre foram submetidos às soluções hidroalcoólicas (0 a 100%) de corantes têxteis adquiridos em mercados locais. A solução hidroalcoólica a 50% dos corantes mostrou maior eficiência no contraste dos tecidos, maior solubilidade do pó corante e melhor interação das soluções com os tecidos vegetais. A maioria dos corantes testados mostraram resultados satisfatórios. A parede celular, especialmente a lignificada, mostrou maior eficiência de coloração. Análises de ancoragem molecular utilizando modelos de celulose e lignina mostraram os prováveis mecanismos de associação e seletividade dos corantes com os componentes da parede celular. A abordagem aqui realizada pode ser útil em aulas práticas conjugadas de anatomia vegetal, química e / ou bioquímica, tanto no ensino médio quanto no nível de graduação.

Palavras-chave: química computacional, metodologia acessível, anatomia vegetal, método de coloração, corantes têxteis.

[1] Universidade Federal de São João Del-Rei, Lab. Anatomia Vegetal, Depto. Ciências Exatas e Biológicas, *Campus* de Sete Lagoas, R. Sétimo Moreira Martins 188, Itapoã, 35702-031, Sete lagoas, MG, Brazil.

[2] Universidade Federal de São João Del-Rei, Lab. Modelagem Molecular e Bioinformática (LAMMB), Depto. Ciências Exatas e Biológicas, *Campus* de Sete Lagoas, R. Sétimo Moreira Martins 188, Itapoã, 35702-031, Sete lagoas, MG, Brazil.

[3] ORCID: <https://orcid.org/0000-0001-6616-6538>

[4] Author for correspondence: cleberjs@ufsj.edu.br

Introduction

Plant anatomy is an important tool to allow a realistic interpretation of morphology, physiology, and phylogeny and to understand ecological processes. It has been proved the most useful in combined studies to better understand the phylogenetic relationships between different plant groups. Furthermore, knowledge of plant structure is essential to address many important everyday problems such as the identification of unknown food contaminants and forensic problems (Metcalfe 1961; Yeung 1998; Dengler 2002; Bock & Norris 2016).

One of the main methods for studying plant anatomy is the analysis of thin and transparent tissue sections. This facilitates the observation and interpretation of plants' tissues (Macedo 1997). The interpretation of any colorless plant material can be improved by the application of dyes to provide contrast between tissues, facilitating their visualization under optical microscopy and revealing their specific cell structures (Kierman 1990; Kraus & Arduim 1997).

Dyes are substances that impart color to a substrate via a process that alters any crystal structure of colored substances. Dyes are classified according to their application and chemical structure. They comprise a group of atoms known as chromophores, which are responsible for the dye color. These chromophore-containing centers have diverse functional groups such as azo, anthraquinone, methine, nitro, aril-methane, and carbonyl (Dos Santos *et al*. 2007; Arun & Bhaskara 2010; Bafana *et al*. 2011).

Staining generally occurs via physical and/or chemical processes. Dyes can be grouped into three classes: dyes that stain the acidic and basic cell components, specialty colorants, and metal salts (Gartner & Hiatt 1999; Geneser 2003; Rohde *et al*. 2006). In histological staining, the most widely used dyes are the basic and acid dyes that react, respectively, with cell acidic and basic components (Walwyn *et al*. 2004).

Traditionally, various synthetic dyes have been used for staining plant structures, for instance, alcian blue, safranin, toluidine blue, fast green, crystal violet, iodine green, Congo red, and neutral red (Dop & Gautié 1928; Kirk 1970; Bukatsch 1972; O'Brien & McCully 1981). Most of these dyes can be expensive and produced by specific companies.

Studies have attempted to use alternative dyes in histological studies in animals (Rohde *et al*. 2006); however, to our knowledge, no study has reported the use of alternative dyes in plant anatomy analysis. Thus, studies on identifying alternative dyes that are affordable for students and teachers at various education levels might facilitate and widen the scope of plant anatomy studies.

Textile dyes are listed as the most hazardous industrial pollutants; they are highly visible and undesirable in effluents even in very low concentrations (Robinson *et al*. 2001; Hubbe *et al*. 2012; Vikrant *et al*. 2018). In fact, the complete degradation of chemicals commonly used in such dyes involves onerous and expensive processes, and water and soil pollution caused by their occasional discharge in effluents is a critical environmental problem at a global scale (Khan & Malik 2018; Vikrant *et al*. 2018). Thus, new alternative applications of such dyes need to be explored while considering the economic and environmental sustainability (Marcucci *et al*. 2001; Granato *et al*. 2017).

Therefore, this study aimed to develop a low-cost and environmentally promising alternative by using textile dyes that can interact with plant tissues, to create contrast between cell structures. In addition to testing the efficiency of alternative textile dyes for staining anatomical sections, we elucidated the molecular mechanisms of interaction of representative compounds commonly found in dyes to develop computational models of archetypal cell wall polymers (crystalline cellulose and lignin models) by using virtual docking methodologies (Martínez *et al*. 2010; Yuriev *et al*. 2015).

Our results corroborate the high potential of using textile dyes for plant tissue staining, as well as the possibility of using both anatomical and computational methodologies for practical and didactic purposes.

Materials and Methods

Plant material

The samples (Tab. 1) were prepared using the common techniques used in plant anatomy studies. Fresh stems, leaves, and roots were sectioned using disposable razors and polystyrene as a support (Ruzin 1999). Wood fragments were macerated using Jeffrey solution (Johansen 1940). Leaf diaphanization was performed according to the technique of Kraus & Arduim (1997).

Sections were cleared in sodium hypochlorite (5%) until they became translucent. Subsequently, they were thoroughly washed with distilled water. Some sections were rinsed in distilled water

Table 1 – Plant material selected to be subject to the staining procedures.

Sample		Leave	Stem	Root	Wood (Macereted)
Angiosperms	Monocots	*Brachiaria* sp. (Trin.) Griseb.[1]	-	*Zea mays* L.[1]	-
	Eudicotyledons	*Caryocar brasiliense* Cambess.[1]; *Amaranthus* sp. L.[4], *Pereskia aculeata* Mill.[3]; *Dendrobium* sp. Sw.[1]	*Tridax procumbens* L.[1]; *Sechium* sp. P. Browne[1]; *Pereskia aculeata* Mill.[2]; *Luffa aegyptiaca* L.[1]	*Capsicum baccatum* 'Pendulum" (Willd.) Eshbaugh[1]	*Eucalyptus* sp. L'Hér.
Gymnosperms		-	-	-	*Pinus* sp. L.

Sections: [1] = transverse; [2] = longitudinal; [3] = paradermal; [4] = Diaphanization

containing drops of acetic acid, as indicated by Macedo (1997), to check for possible improvement in the results.

Preparation of staining solutions

Commercial textile dyes (powder; Tab. 2) were obtained from local markets. The material safety data sheet (MSDS) from the manufacturer suggested that the dyes used in this study were a mixture of pigments containing azo/stilbene groups, without specifying the chemical structure of the dye components. About 10% (weight/volume) of each textile dye in a series of dilutions of hydroalcoholic solution (0%−100%) was prepared at room temperature and heated at 100 ºC. The pH was adjusted to acidic (pH = 4.0) and basic (pH = 11.0). The efficiency of the use of mordants in the interactions of dyes with plant tissues, as proposed by Johansen (1940), was analyzed by adding 0.2 g sodium acetate + 0.4 mL of formaldehyde to the dye solutions. Mordants were also prepared in 3% acetic acid solution.

Staining procedure

The sections were dehydrated in hydroalcoholic solution until the required concentration of dye was achieved. The material was stained for 05−60 min and washed with hydroalcoholic solution at the same concentration of the dye solution with varying pH (4.0 and 11.0; Macedo 1997). Preliminary tests were performed using a mixture of two dyes containing 50% hydroalcoholic solution. The macerated plant material was stored in a dye solution for six days.

Treatment after staining

The dye manufacturers also provide a "fixative" (cross-linked amide resin) that, according to them, "improves the fixation of natural dyeing." This fixative was prepared in 50% hydroalcoholic solution (1:1) and applied for 1 min after staining.

Mounting medium

All preparations were mounted in glycerinated gelatin according to Kaiser (1880) with the following modifications: (i) gelatin (colorless and unflavored) and glycerin were obtained from local markets; (ii) phenol was substituted by five commercial Indian cloves buds (*Syzygium aromaticum* (L.) Merr. & L.M. Perry), and incubation was performed overnight.

Optical analysis and photographic documentation were performed using a microscope *Primo Star Zeiss* coupled to a camera (*Axiocam ERc MRc 5s*) and software *Axiovision documentation*.

Table 2 – Relationship dyes / colors used in the tests.

Manufacturer	Color
Tupy (*Corantes Tupy* line)	*Bordô 16*, *Laranja Califórnia 06*, *Pink 13*, *Roxo 19*, *Verde Primavera 26*
Guarany (*Tingecor* line)	*Amarelo 03*, *Amarelo Ouro 4*, *Azul 17*, *Bege 26*, *Cinza 30*, *Laranja 05*, *Lilás 68*, *Maravilha 08*, *Marinho 16*, *Natier 15*, *Preto 31*, *Turquesa 13*, *Verde 20*, *Vermelho 09*, *Violeta 25*, *Vinho 61*

Computational chemistry

Computational chemistry based on structural modeling and virtual docking was used to obtain insights about the fixing mechanisms of the major constituents (*i.e.*, canonical stilbene/azo pigments) of the dyes used in this study to representative cell wall constituents.

Microcrystalline cellulose and racemic lignin models

The microcrystalline cellulose I-β model (Matthews *et al*. 2006) was generated using the Cellulose Builder package (Gomes & Skaf 2012); it consisted of three (1:1:1) monolayers of cellulose fibrils with approximate dimensions of 8 × 45 × 60 Å. Cellulose Builder is an optimized software to generate models of cellulose crystallites of arbitrary size in XYZ coordinates and PDB formats (Gomes & Skaf 2012).

For lignin, three different models were generated to determine the significant representativeness of different subconformations and chiral configurations for this amorphous and racemic polymer. Three preliminary and racemically distinct models following the canonical softwood lignin depiction (Sakakibara 1980; Petridis *et al*. 2011) were generated using software Avogadro (Hanwell *et al*. 2012). Since no "specialized" software is available to generate lignin models, Avogadro was chosen owing to its versatility both in the generation as well as optimization of complex molecular models at a relatively low computational cost (Hanwell *et al*. 2012). As described in the literature (Sakakibara 1980; Petridis *et al*. 2011), these models presented a random distribution of chirality at the bonds connecting the three equally canonical monomers (paracoumaryl, coniferyl, and sinapyl alcohols). These initial models were first subjected to a in vacuum energy minimization protocol by using a conjugated gradient (in order to eliminate local clashes and/or distortions) with the UFF force field (Rappé *et al*. 1992), followed by geometrical optimization by using the same software by using software default rotamer search algorithm. Three higher models were also generated using random crosslinking of the C-O-C and C-C extremities of the abovementioned initial units, according to the canonical softwood model (Sakakibara 1980). The approximate C:H:O ratio and molecular formula for these higher models were 3:3:1 and $(C_{31}\,H_{34}\,O_{11})_{26}$, respectively. Therefore, a solvation layer, containing 25.000 water molecules within a 50 Å radius, was added to the models by using PACKMOL software (Martínez *et al*. 2009). PACKMOL was used because it could generate reliable models of heterogeneous molecular systems respecting spatial constraints that ensure no repulsive interactions (Martínez *et al*. 2009). A final energy minimization and conformational optimization were performed for these solvated models, by using Avogadro and the UFF, resulting in three final and optimized lignin.

Molecular docking

Virtual molecular docking studies of stilbenes and azo dyes on the three-dimensional models of microcrystalline cellulose I-β and amorphous lignin were performed using Autodock Vina software (Trott & Olson 2010). This software was already used successfully in a previous study investigating the affinity of olignol-derived adhesives with a microcrystalline cellulose I-β model (Martínez *et al.* 2010). A total of 37 compounds of these respective classes commonly found in textile dyes were selected from Zinc virtual Database (Irwin *et al*. 2012) or built-in Avogadro software; they included the following: 22 non-stilbene azo compounds (4-Aminobiphenyl (*Azo1* with ZINC38338719); benzidine (*Azo2*, ZINC00265747); 4-chloro-o-toluidine (*Azo3,* ZINC157577); 2-Naphthylamine (*Azo4*, ZINC00968125); 4-amino-2,3-dimethylazobenzene (*Azo5*, ZINC3860960); 2-amino-4-nitrotoluene (*Azo6*, ZINC01648344); 4-Chloroaniline (*Azo7*, ZINC00403225); 2,4-diaminoanisole (*Azo8*, ZINC00406912); 4,4-diaminodiphenylmethane (*Azo9*, ZINC19014778); 3,3-dichlorobenzidine (*Azo10*, ZINC57298); 3,3-dimethoxybenzidine (*Azo11*, ZINC38219021); 3,3-Dimethylbenzidine (*Azo12*, ZINC56751); 3,3-dimethyl-4,4-diaminodiphenylmethane (*Azo13*, ZINC78247); 4-cresidine (*Azo14*, ZINC157578); 4,4-methylene-bis-2-chloroaniline (*Azo15*, ZINC56414); 4,4-oxydianiline (*Azo16*, ZINC260472); 4,4-thiodianiline (*Azo17*, ZINC225617); 2-aminotoluene (*Azo18*, ZINC1706910); 2,4-diaminotoluene (*Azo19*, ZINC00388039); 2,4,5-trimethylaniline (*Azo20*, ZINC01680827); 2-methoxyaniline (*Azo21*, ZINC00404293); 4-aminoazobenzene (*Azo22*, ZINC18060741); one azo stilbene compound in *cis* configuration and disulfonated (4,4-diaminostilbene-2,2-disulfonic (*AzoStcis*, ZINC12339511); three azo stilbenes in configuration *trans* (4-Methoxy-4-nitrostilbene (*AzoStTr1*, ZINC186928); DIDS

(*AzoStTr2*, ZINC6844860); SITS (*AzoStTr3*, ZINC3915614), *being both compounds AzoStTr2 and AzoStTr3 also bi-sulfonated*); four non azo stilbenes in *cis* configuration (E-stilbene-cis (*StilCis1*, ZINC8585877); combretastatinA-4 (*StilCis2*, ZINC13452167); dienestrol (*StilCis3*, ZINC00001283); Z-3,5,4-trimethoxystilbene (*StilCis4*, 00009252) and six non azo stilbenes in *trans* configuration (E-stilbene-trans (*StilTr1*, ZINC1577148); 3,5,4-Trihydroxy-trans-stilbene (*StilTr2*, ZINC00006787); diethylstilbestrol (*StilTr3, ZINC00001290*); E-3,5,4-Trimethoxystilbene (*StilTr4*, ZINC13456778); 1,4-Bis4-Methylstyrylbenzene (*StilTr5*, ZINC02556773); pterostilbene (*StilTr6*, ZINC00899213). This selection provided a considerable variance in the physicochemical parameters for surface interactions and adsorption: polarity, geometry (linear or angular), number of aromatic rings (between 1 and 3), size, and contact surface. All the virtual docking procedures were performed in triplicate, both for the single model of micro-crystalline cellulose as well as for each one of the three amorphous models of lignin. In all the cases, the docking grid included all the models, with a minimum padding of 2 Å and a maximum of 5 Å. No flexibility was assumed for any group of polymeric models during the docking assays. All remaining docking parameters were configured and set as the software default. Although the docking box was relatively large, the exhaustiveness parameter was maintained at the default of 8. This is not expected to have compromised the accuracy of the findings considering the better docking poses recovered in the present study. First, the microcrystalline cellulose model presents a homogenous surface that significantly limits the number of possible binding modes of each ligand. In contrast, our small lignin models, although amorphous and more heterogeneous, present binding cavities along the surface with relatively short extensions, again limiting the number of favorable possibilities for the more energetically permissive poses. Finally, rather than recovering an exact view of all the possibilities of binding modes for these relatively non-specific interactions, this study intended to recover a comparative and semi-quantitative view of the major molecular attributes that orchestrate the association of these classes of ligands with each one of the cell wall polymers. The final docking scores considered for microcrystalline cellulose model were the respective averages from the five best poses at each of the three docking assays (totaling an average of 15 poses per ligand). For the amorphous lignin models, the average of the five best poses was considered for each triplicate considering each one of the three respective softwood approximated models (totaling an average of 45 poses per ligand). The significantly higher statistical value considered for lignin docking was necessary, because of the higher conformational freedom for this polymer unlike microcrystalline cellulose.

Results

The dyes' interactions with plant tissues are shown in Tables 3 and 4 and Figures 1-5. The best staining time was 40 min for *Azul 17*, *Maravilha 08*, *Marinho 16*, *Vermelho 09*, *Vinho 61*, and *Violeta 25* and 60 min for the others. Variations in color and contrast between tissues, related to alcohol solution concentration, exposure time, and dye interaction with plant material, were observed. Therefore, adjusting according to the material and the desired staining intensity was necessary, as observed in Figure 1.

The 50% hydroalcoholic solution remarkably improved the solubility of the dye powder and facilitated better interaction of the solution with the plant tissue. The pH alteration had no influence on the results. Similarly, the temperature of the solutions did not influence the powder dyes' solubility and the final staining results.

Freehand sections that were washed with distilled water and drops of acetic acid after the clarification process, as suggested by Macedo (1997), did not show improved staining. Similarly, the variation in pH (4.0 and 11.0) of the wash solutions after staining did not have significant influences on the staining results.

The post-staining treatment with the "fixative" was found to be effective to prevent the migration of the dyes to the glycerinated gelatin.

Intense staining in the lignified secondary walls was noted. The staining was less intense in the collenchyma. In the thin primary cell walls of parenchyma, less interaction of the dye was noted. The dyes *Preto 31*, *Turquesa 13*, *Pink 13*, and *Verde Primavera 26* did not interact with the plant tissues.

The dyes *Lilás 68* (Fig. 2b), *Laranja 05* (Fig. 2c), *Marinho 16* (Fig. 4c), *Violeta 25* (Figs. 4f, 5f,h), *Azul 17* (Fig. 5d), and *Vermelho 09* stained both the thickened primary walls of the collenchyma as well as the lignified walls (fibers, xylems, and sclereids). Moreover, the dyes Bege 26 (Fig. 2d), *Amarelo 03* (Fig. 2g), *Verde 20* (Fig.

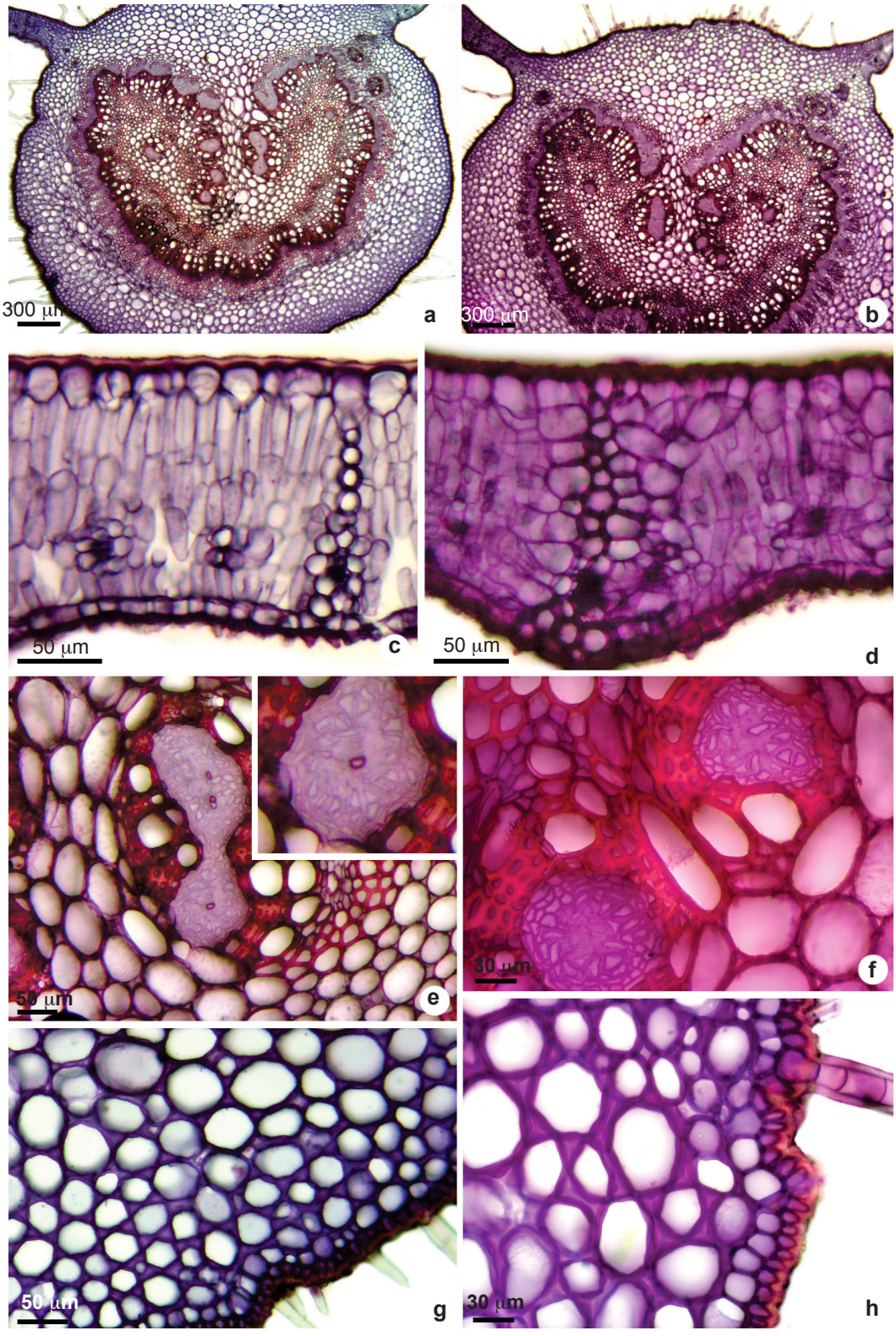

Figure 1 – a-h. Leaves of *Caryocar brasiliense* staining with *Marinho 16* in hydroalcoholic solution 20% (a, c, e, g) and 50% (b, d, f, h) – a-b. midrib region; c-d. mesophyll; e-f. detail of concentric vascular bundle of midrib; g-h. collenchyma detail of the midrib region.

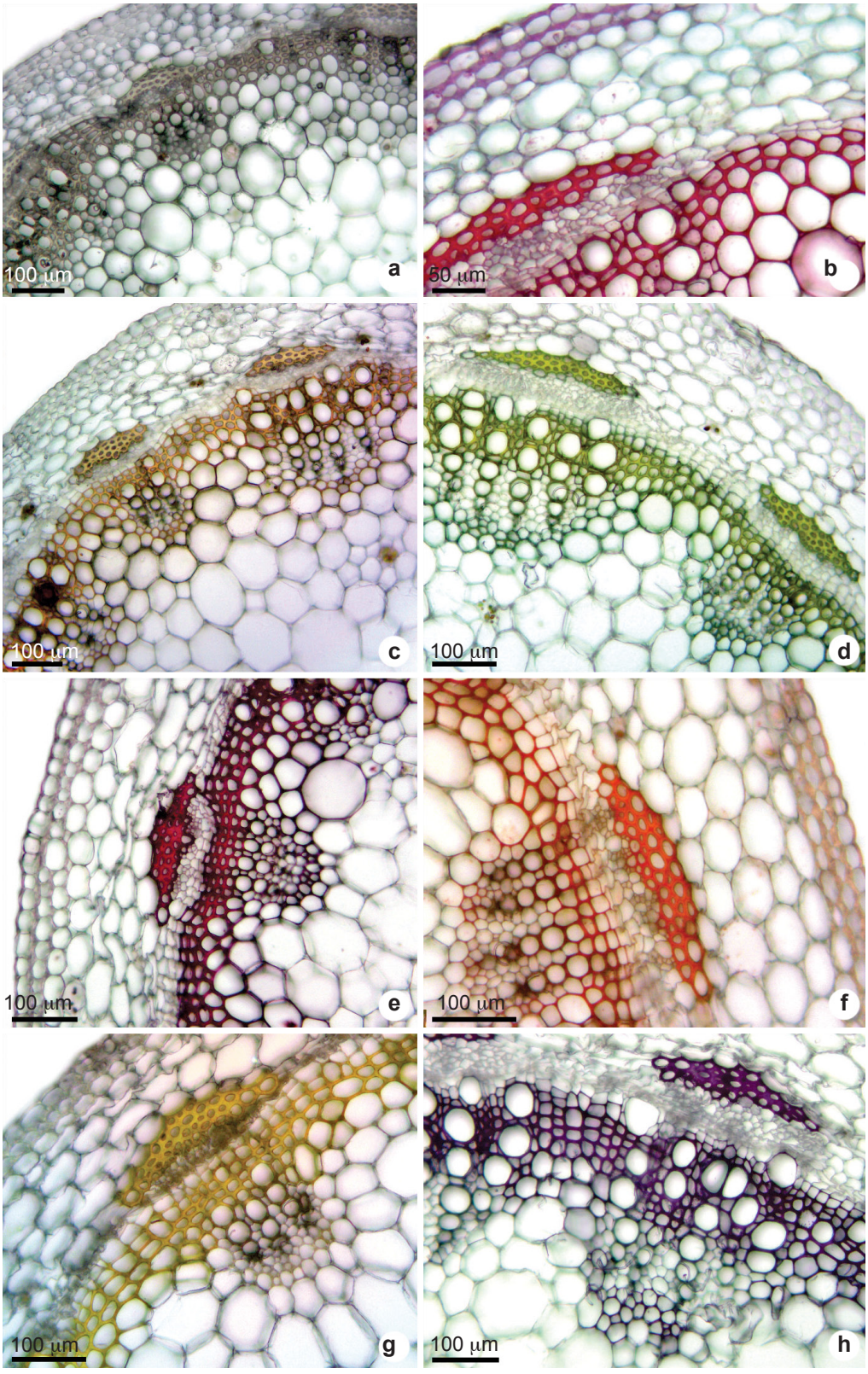

Figure 2 – a-h. Stem of *Tridax procumbens* in cross section staining with hydroalcoholic solution 50% – a. unstaining; b. *Lilás 68*; c. *Laranja 05*; d. *Bege*; e. *Verde 20*; f. *Vinho 61*; g. *Amarelo 03*; h. *Natier*.

Table 3 – Interaction of dyes with plant tissues - *Guarany* (*Tingecor* line)

Dye	Thin primary wall	End color	Primary thickened wall (collenchyma)	End color	Secondary wall	End color
Amarelo 03	-	-	-	-	+++	yellow
Amarelo Ouro 4	-	-	-	-	+++	yellow
Azul 17	+++	light blue	+++	blue	+++	intense red
Bege 26	-	-	-	-	+++	light brown
Cinza 30	-	-	-		+++	light wine
Laranja 05	+	orange light	++	orange	+++	orange dark
Lilás 68	-	-	++	pink	+++	intense red
Maravilha 08	-	-	-	-	+++	red intense
Marinho 16	+++	light blue	+++	purplish blue to lilac	+++	intense red
Natier 15	-	-	-	-	+++	purple
Preto 31	-	-	-	-	-	-
Turquesa 13	-	-	-	-	-	-
Verde 20	-	-	-	-	+++	dark yellowish green
Vermelho 09	+	orange light	++	orange	+++	orange dark
Violeta 25	+	light violet	++	light violet	+++	dark violet
Vinho 61	-	-	-	-	+++	dark wine

2e), *Vinho 61* (Fig. 2f), *Nátier 15* (Figs. 2h, 4d), *Laranja Califórnia 06* (Fig. 4b), *Bordô 16* (Fig. 4g), *Roxo 19* (Fig. 4h), *Amarelo Ouro 04*, *Cinza 30*, and *Maravilha 08* interacted intensely with lignified secondary walls. The color patterns produced by the interaction of the dyes with plant tissues are shown in Tables 3 and 4.

Slight precipitation of the dyes was noted after application at the plant tissues; this was visible only under the 40x objective lens of a microscope. Precipitate formation occurred when the dye application was performed in watch glasses. In contrast, when the dyes were applied in closed containers, no precipitate formed.

The staining durability of the dyes on microscope slides prepared using glycerinated gelatin was a minimum of seven days and a maximum of three years.

Table 4 – Interaction of dyes with plant tissues - *Tupy* (*Tupy* line).

Dye	Thin primary wall	End color	Primary thickened wall (chollenchyma)	End color	Secondary wall	End color
Bordô 16	-	-	-	-	+++	red
Laranja Califórnia 06	+	red light	-	-	+++	red intense
Pink 13	-	-	-	-	-	-
Roxo 19	+	red light	-	-	+++	red intense
Verde Primavera 26	-	-	-	-	-	-

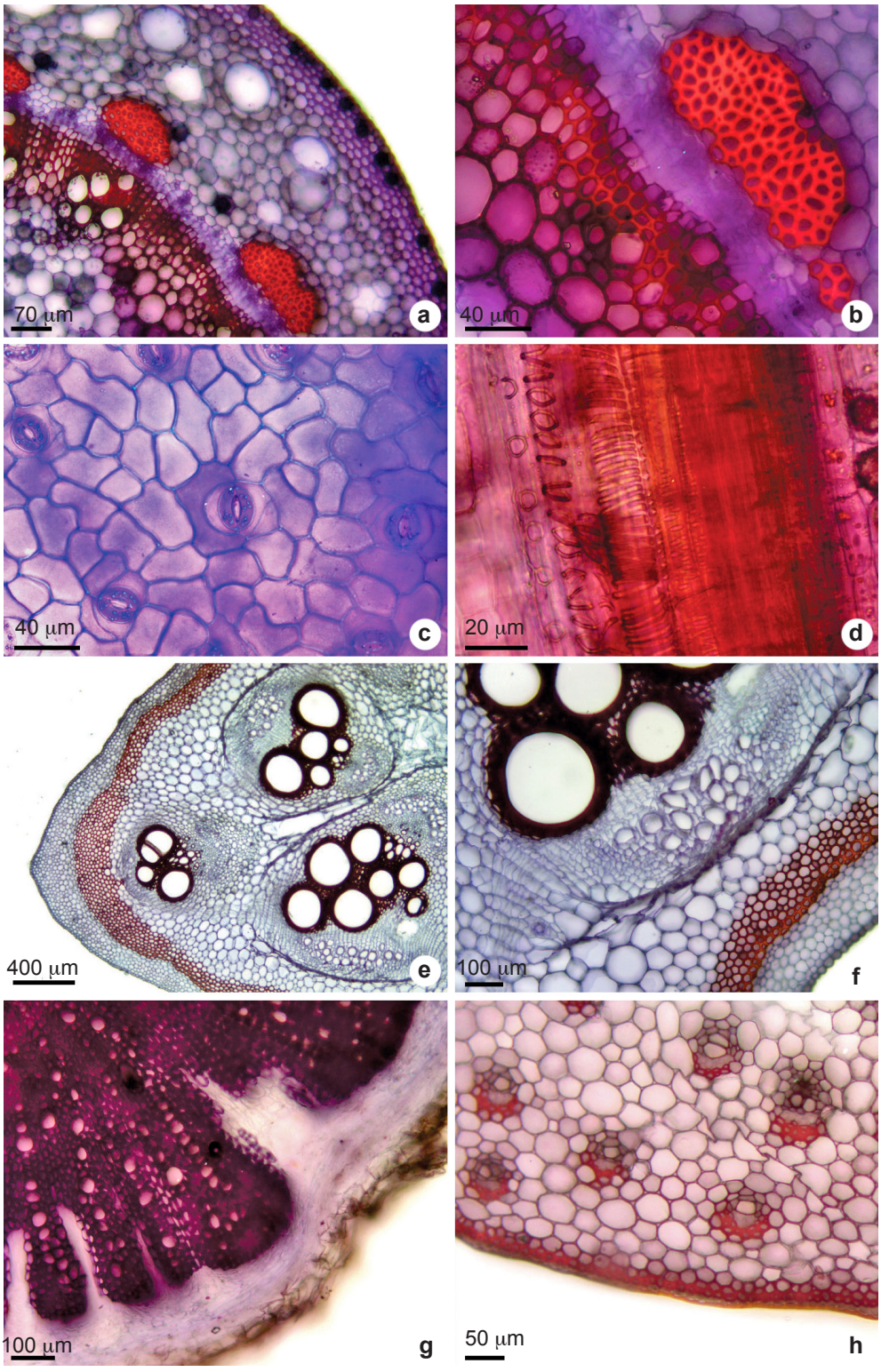

Figure 3 – a-h. Double staining with hydroalcoholic solution 50%. a-b. *Pereskia aculeata* staining with *Laranja 05* x *Marinho 16* (Stem in cross section)– a-b. stem in cross section; c. leave in paradermic section; d. stem in longitudinal section; e-f. cross section of *Luffa aegyptiaca* stem in *Laranja 0*5 x *Marinho 16*; g. cross section of *Capsicum baccatum* 'Pendulum' root in *Lilás 68* x *Marinho 16*; h. cross section of *Dendrobium* sp. stem in *Laranja 05* x *Marinho 16*.

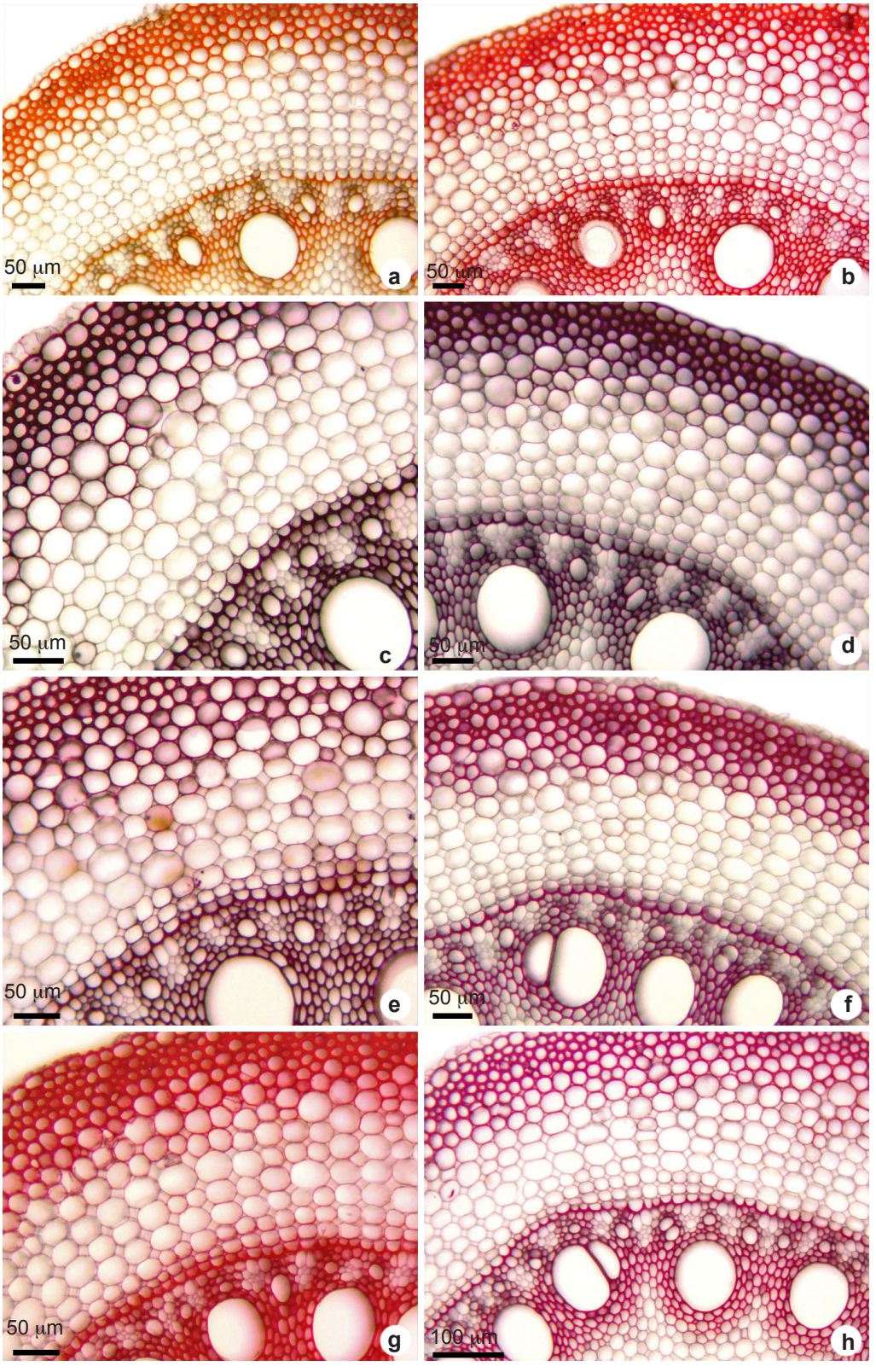

Figure 4 – a-h. Root of *Zea mays* in cross section staining with hydroalcoholic solution 50% – a. *Laranja*; b. *Laranja Califórnia*; c. *Marinho 16*; d. *Natier*; e. *Vinho*; f. *Violeta 25*; g. *Bordô*; h. *Roxo 19*.

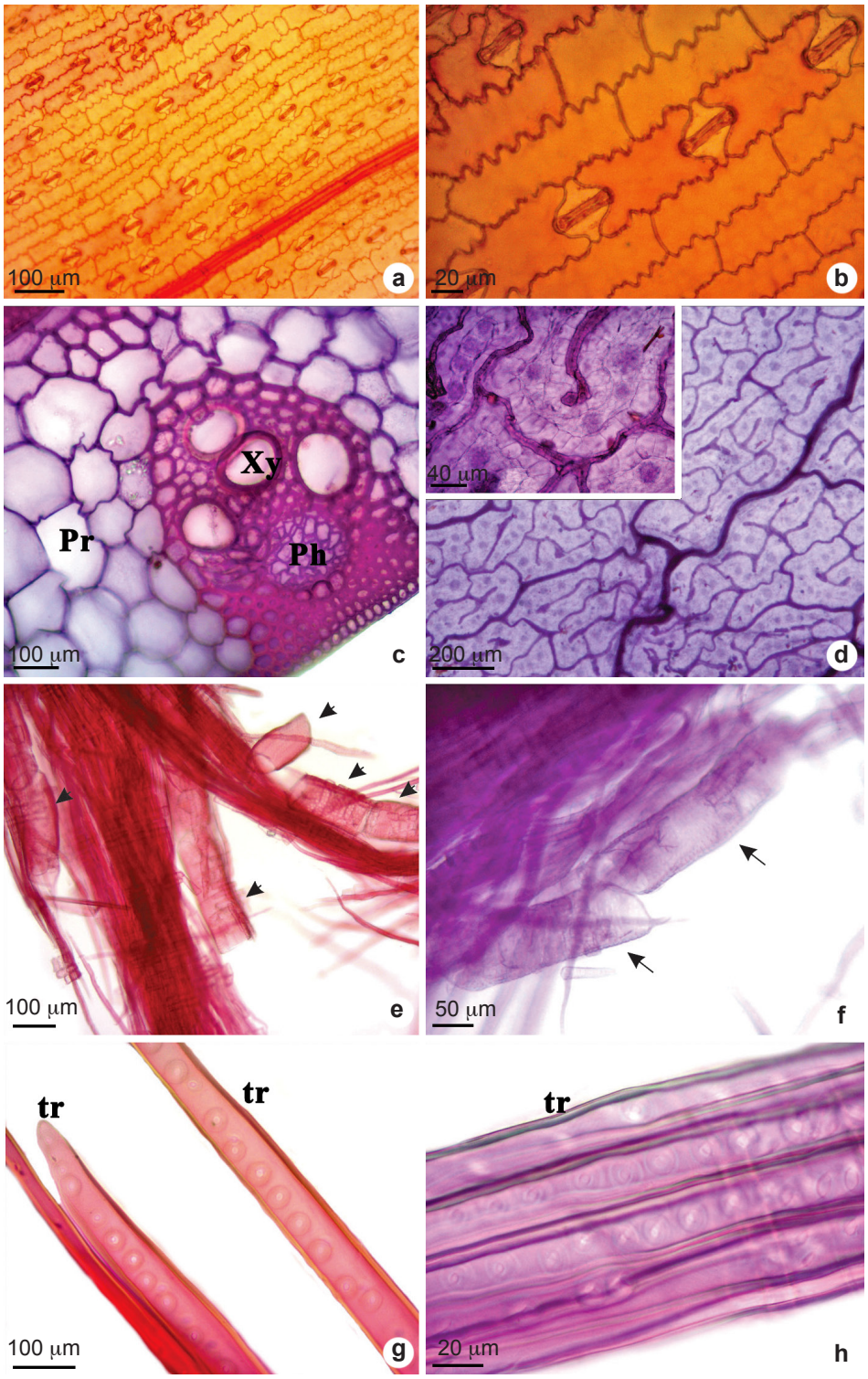

Figure 5 – a-h. Sections staining with hydroalcoholic solution 50% – a-b. leaf of *Brachiaria* sp. in parademic section stained with *Maravilha* x *Amarelo Ouro*; c. leaf of *Brachiaria* sp. in transversal section stained with *Marinho 16*; d. leaf of in *Amaranthus* sp. stained with *Azul 17* (diaphanization); e-f. macereted of wood of *Eucalyptus* sp. stained with *Bordô* (e) and *Violeta* (f); g-h. tracheids in the macereted of wood of *Pinus* sp. stained with Bordô (g) and *Violeta* (h). Xy = xylem; Ph = phloem; tr = tracheids.

The preliminary test with the mixture of two dyes in 50% hydroalcoholic solutions revealed promising results. The final staining showed good contrast between tissues (Figs. 2i-k, 6), indicating the possibility of using different combinations of dyes for double-staining by using this technique.

The modified glycerinated gelatin was found to be a suitable mounting medium, preserving the vegetal material for more than three years, without any damage due to the action of fungi, bacteria, or insects.

The staining profiles of different plant tissues described above showed high affinity of the dyes' pigments to cell wall polymers, especially to lignified tissues. To obtain insights about the molecular basis of such effects (as well as the possibilities of how to optimize the process of selective staining by using textile dyes in future studies), we performed virtual docking experiments for representative stilbene/azo pigments by using structural models of crystalline cellulose surface and lignin fragments.

In all the cases, structural analysis of the binding modes recovered during the virtual docking experiments suggested that the interactions of the dye molecules with the polymer surfaces were mainly attributed to π interactions and hydrogen bonds (in the case of polar-substituted ligands; (Figs. 6-7). A considerable range of ligands' energetic docking score values were noted for both polymers, ranging from -2.70 (less favorable score in cellulose) to -8.90 kcal mol^{-1} (more favorable score in lignin; Fig. 8). Consistent with the binding modes shown in Figures 6 and 7, two respective attributes showed higher significance to differentiate the ligand-polymer affinity: the ligand polarity (represented by the dipole moment in Debye units) and an arbitrary and discrete scale of "geometric factor." This last geometric factor (GF) scale was then idealized in order to increase according to the respective enhancement in the ligand surface-accessible area that can establish simultaneous π interactions with the polymer surface and/or cavities (in the case of lignin). In particular, for the stilbene/azo compounds investigated in this study, the arbitrary GF defined is the function of both geometric adjustments (linear configurations being more favored that extended ones) as well as the elongation of the ligand major axis and/or increasing of the hyperconjugation degree. Highlighting that this arbitrary/discrete GF scale is only valid for the "canonical" geometries of the stilbene and azo classes, respectively, is necessary.

For cellulose, a polar, non-aromatic polymer, the major binding modes recovered in this study resided in two major subtypes of interactions. Structural analysis suggested that the nonpolar ligands interact by C-H-π stacking with the cellulose-CH groups (Fig. 6b-e). However, in the case of polar-substituted dyes, the ability of the same to position the polar groups in the grooves between the fibrils is crucial to the establishment of strong hydrogen interactions with the sugar -OH groups, as well as with the oxygen molecules from the rings and glycosidic bonds (Fig. 6c,e). This similar dependence of ligand affinity on its ability to establish both π interactions as well as hydrogen bonds with the cellulose surface reflects in the more negative docking scores (Fig. 8a) for ligands that also present high geometric factors and high dipole moments.

In contrast, lignin seems to favor the association of most of the binders compared to cellulose, returning energetic docking scores significantly more negative than the last (Fig. 8b). This is in considerable concurrence with the higher ability of the majority of the dyes experimentally investigated in this study to stain more lignified tissues compared to the less lignified ones (as related at the last topic). This relative higher average affinity seems to be related to the higher ability of the lignin polymer - amorphous, rich in hydrophobic cavities, and (overall) with polyaromatic constitution (Sakakibara 1980; Petridis *et al.* 2011) - to establish π aromatic interactions with the ligands (Fig. 7b-d). This can be verified both by the considerably higher direct dependence of the docking score for this polymer on the geometric factor comparing the same dependence on cellulose, as well as by the lower dependence of the lignin scores on the intensity of the ligand dipole moment (Fig. 8b). For instance, the *trans*-stilbene derivative with GF 7 (Fig. 7d) presents the highest geometric factor index, but lower dipole moment. This ligand presents, in concurrence with its GF value, a more negative (favorable) average docking score in lignin (-8.9 kcal mol^{-1}), independently of the minor polarity (Fig. 8b). The three sulfonated stilbenes computationally investigated in this study (one of them with its binding mode in lignin depicted in Fig. 7c) presented the highest dipole moments, but intermediate geometric factors (one with factor 4 and two with factor 6). These ligands present relatively less negative docking score values compared to those with factor 7 (Fig. 8b). The scores for these ligands are comparable with those

of their respective less polar counterparts with similar geometric factors. This confirms the minor participation of polar interactions and the higher participation of multiple π interactions in ligand-lignin associations for the dye classes analyzed in this study.

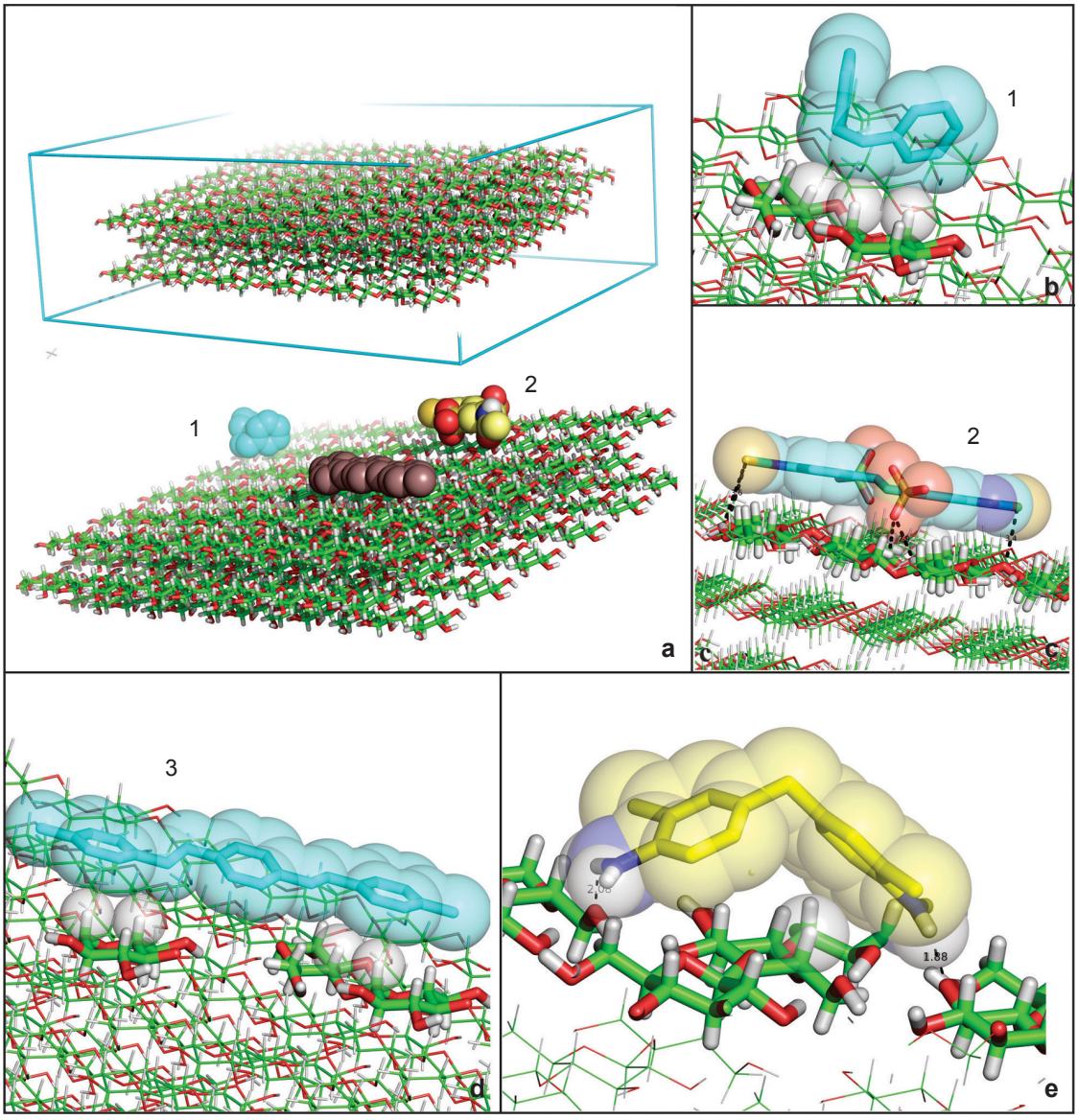

Figure 6 – a-e. General view of the virtual docking experiment and major interaction modes of representative ligand poses for microcrystalline cellulose model – a. top - docking box involving all the microcrystalline cellulose I-b model; a. bottom - poses of three representative stilbene derivatives (numbered 1, 2 and 3) docked over the same model at the same docking box; b-d. interaction modes of the best poses of the respective three ligands 1 (StilCis1, ZINC8585877), 2 (AzoStTr2, ZINC6844860) and 3 (StilTr5, ZINC02556773) are showed. Receptor hydrogens involved in C-H-----π interactions are shown as Van der Waals spheres marked with a red asterisk. Hydrogen bonds between respective polar groups of the ligand and the receptor are depicted as dashed lines in c. and d.; e. angular and polar azo derivative (Azo9, ZINC19014778) showing the hydrogen bonds intercalated between the fibers (dashed lines) that this class is able to stablish specifically at the cellulose interaction, beyond the single C-H----π interaction (hydrogen in Van der Waals sphere and with red asterisk).

Discussion

The interaction of textile dyes with cellulose and lignin in plant tissues occurred satisfactorily, as expected, since they are largely used in the textile industries to stain cotton and other natural or synthetic fibers (Villalobos *et al*. 2016; Ajmal *et al*. 2016; Rayati & Sheybanifard 2016).

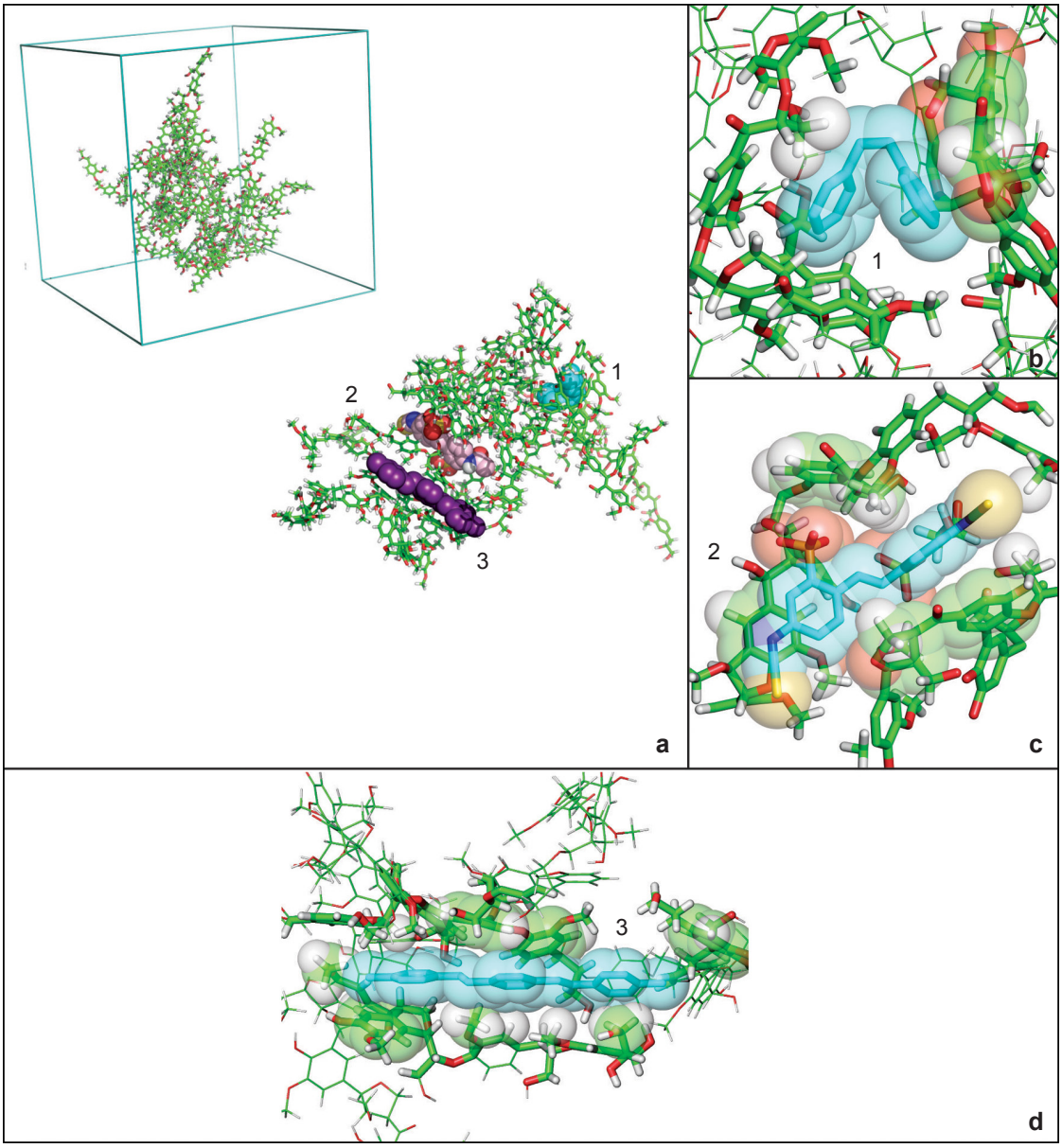

Figure 7 – a-d. General view of the virtual docking experiment and major interaction modes of representative ligand poses for softwood lignin model – a. top - docking box involving all the representative lignin model; a. bottom - poses of three representative stilbene derivatives (numbered 1, 2 and 3) docked over the same model at the same docking box; b-d. interaction modes of the best poses of the respective three ligands 1 (StilCis1, ZINC8585877), 2 (AzoStTr2, ZINC6844860) and 3 (StilTr5, ZINC02556773) are showed. It can be noted the more significant entrapment of the ligand by the lignin cavities compared to the planar microcrystalline cellulose (Fig. 6) and the higher contribution of the aromatic, hydrophobic and C-H-----π interactions (the hydrogens involved in these last showed as Van der Waals spheres marked with a red asterisk).

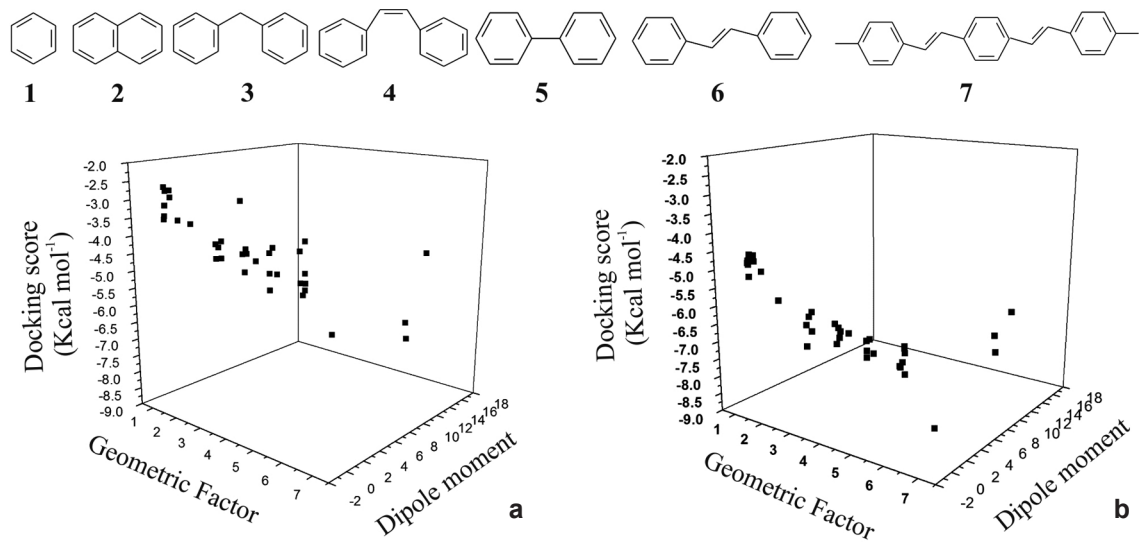

Figure 8 – a-b. Relationship between average docking score and ligand attributes for the two types of cell wall polymers. At the *top* is depicted an arbitrary scale of "Geometric Factor" measure that grows according to the ability of the ligand to maintain simultaneous π stacking interactions with the polymer – a. three dimensional relationship between cellulose docking score *Vs* ligand geometric factor *Vs* ligand dipole moment in Debyes (D); b. the same three-dimensional relationship for softwood lignin models.

The MSDS from the manufacturer informed that the dyes used in this study are a mixture of pigments from the azo/stilbene groups, without specifying the chemical structure of the dye components. However, information about the common chemical properties of azo/stilbene derivatives (Kierman 1990; Yousefi *et al*. 2013), as well as our experimental and computational data, allowed the inference of some probable mechanisms in which these commercial dyes could selectively stain plant tissues. For instance, the best solubility experimentally found for the dyes mixed with 50% hydroalcoholic solution might be attributed to the chemical structural groups usually found in these compounds. In fact, the majority of the 37 representative compounds of these classes randomly selected in this study from the zinc database (Irwin *et al*. 2012) commonly showed both hydrophobic (aromatic) regions and polar groups. This intermediary polar/apolar nature could have been responsible for the recovered interaction modes in the computational molecular docking assays for microcrystalline cellulose. Thus, not surprisingly, the dyes compounded with mixtures of pigments of these classes showed maximum solubility in solutions with intermediary polarity (as is the case of 50% hydroalcoholic solution). However, information on the solubility of textiles dyes is limited. According to Leal (2011), although considerable studies have been performed on dyes, surprisingly, a fundamental thermodynamic property - solubility - has been little investigated. The azo compounds carry the azo group (-N = N-) as a chromophore, which connects two aromatic systems, and form a staining class having many practical applications (Kierman 1990; Yousefi *et al.* 2013). They provide bright, strong color shades varying from red to green and blue (Yazdanbakhsh *et al*. 2010; Geng *et al*. 2011); are stable in light; resistant to chemical and microbial attacks; and have superior fixing quality (Adedayo *et al*. 2004; Forss & Welander 2011). We found that this set of characteristics can be favorably used to provide contrast in optical microscopy analyses of plant tissue sections. Several studies have hypothesized the interactions between cellulose and these and other dyes. Ladchumananandasivam & Miles (1994) suggested that dyes could adsorb onto the surfaces of crystalline nano-domains in cotton. Kreze *et al.* (2002) suspected that dyes, depending on their molecular size and solubility characteristics, might permeate into the amorphous regions of cellulose, and Timofei *et al.* (2002) concluded that both crystalline and amorphous cellulose sites are likely to bind with dye molecules. In our computational analysis, a binding mechanism based on surface

-CH-π interactions and hydrogen bonds with the polar groups between the fibrils corroborates the hypothesis of Ladchumananandasivam & Miles (1994) and Timofei *et al.* (2002). However, the greater surface contact of the ligands in the virtual assays on the cavities of the amorphous lignin models (and the higher dissociation energies involved), as well as the higher anatomical staining experimentally verified for tissues richer in this amorphous polymer are also considerably consistent with the hypothesis of Kreze *et al.* (2002). Future computational studies with amorphous cellulose models, as well as more refined experiments in which the selectivity of different isolated pigments to tissues richer in microcrystalline or amorphous cellulose needs to be verified could help in the better elucidation of this issue. All the textile dyes assessed in these studies could stain the tissues without the help of a mordant (substance used to bind the dye to the substrate) and hence are classified as "direct" dyes. The most common direct dyes are usually aromatic substances containing side groups that tend to ionize. Many direct dyes tend to carry a negative charge, and this ability has already been shown to have positive results in the staining of biological tissues (Isenmann 2013). In fact, in our computational models, the negatively charged sulfonated azo-stilbenes had higher affinity to the microcrystalline cellulose surface, corroborating this experimental observation. Even our findings suggest that a crucial factor for the interaction of polar and charged dyes with microcrystalline cellulose is the ability to intercalate their polar/charged substituents between the fibrils, in order to establish hydrogen bonds with the hidden hydroxyl groups. Hence, a strong participation of ligand geometry at the affinity and selectivity of such polar/charged direct dyes (*i.e.*, ligands with respective geometries that allow more adequate positioning of the polar groups between fibrils could, in principle, provide more significant staining) would be expected. A similar behavior was observed in other virtual docking studies for the affinity of oligolignol-derived adhesives to microcrystalline cellulose (Martínez *et al.* 2010). This suggests that these are the common determinants for the affinity of small ligands to crystalline cellulose, which, in turn, can be used in future studies for optimizing the intensity and selectivity of staining.

The intense staining of lignin observed for most of the dyes was in accordance with the findings of Hubbe *et al.* (2012), who suggested that the relatively hydrophobic character of lignin and the many aromatic groups can be useful in the sorption of dyes and a set of other relatively hydrophobic molecules. This is significantly corroborated by our findings of virtual molecular docking analyses. These findings suggest that not only the hydrophobicity and poly-aromaticity of lignin, but also its amorphous configuration, which is rich in cavities with considerable contact surface, are the determinants for the significantly higher affinity for the dyes investigated in this study, compared to cellulose. Drnovsek & Perdih (2005) suggested the reasons for the affinity of dyes; for lignin, some of the lignin phenolic groups placed at the fiber-water interface ionize in contact with cationic dyes to enable a strong ionic interaction. However, in the same study, several, if not most, of the lignin phenolic groups were shown to interact with non-ionized acidic groups, *i.e.*, by donating hydrogen to form hydrogen bonds with electron-rich groups in the dyes. This non-intrinsic dependence of ionization processes at the lignin-dye affinity was confirmed in our staining experiments by the verified poor influence of pH on staining by the majority of the mixtures. Further, in the computational docking analyses, considerable participation of aromatic interactions verified for the pigments' association with lignin models suggested that polar-polar interactions might not be involved in the association of these non-ionized groups. Further, considering polar-π and/or cation-π interactions are important in the interaction of the polar or ionized dyes, given the significance of π-conjugated groups recovered for the interactions by using the lignin models in our computational analysis and the known importance of polar/ion-π interactions in biological systems (Martínez & Iverson 2012; Kumar *et al*. 2018).

The application of the commercial "fixative" during the post-staining treatment did not cause the migration of the dyes to the gelatin glycerin. In the staining processes for textile fibers, fixatives are substances used to create a bridge between the dye molecules and fibers in order to prevent the migration of the dye from the interior of the fiber to the external environment (Peruzzo 2003). The MSDS from the manufacturer provided little information about the compounds of the fixative. It only informed that the dyes were a crosslinked resin amide. According to Costa (2016), the components of a resin used to provide fabric abrasion resistance properties are simply derived from a combination

of formaldehyde and urea derivatives forming bifunctional species containing reactive methylol groups. In the presence of a suitable catalyst, these species react with cellulosic materials to form stable and relatively strong entanglements ("crosslinks") between cellulose polymer chains.

Regarding durability, although synthetic dyes are superior in terms of color availability, permanency, and light stability (Douissa *et al.* 2014; Chowdhury & Saha 2010), in some plant materials tested, the staining lasted only for a few days. Conversely, the duration was more than three years in other vegetal materials. Thus, the alternative dyes tested might be classified as other dyes used in plant anatomy both as semi-permanents (lasting weeks to months) and permanents (very durable, fading resistant; Kraus & Arduim 1997).

The dye solutions need to be stored in amber bottles in a refrigerator and must be filtered on a filter paper or glass wool periodically, as recommended by Kraus & Arduim (1997).

The application of dyes to plant material in closed containers (*e.g.*, penicillin bottles) is strongly recommended to avoid the formation of precipitate that can compromise the staining result.

The substitution of phenol (hydroxybenzene) by cloves on glycerinated gelatin could avoid the known carcinogenic, cytotoxic, and teratogenic properties of phenol (Bukowska & Kowalska 2003; Roy *et al.* 2015; Jović-Jovičić *et al.* 2016). One of the main components of the essential oil of Indian clove is eugenol (up to 95%; Kegley *et al*. 2010; Milind & Deepa 2011). The clove essential oil and eugenol have been described as having useful acaricidal (Mahakittikun *et al*. 2014), insecticidal (Jumbo *et al.* 2014), antifungal (Xing *et al.* 2012), antimicrobial (Goni *et al.* 2009), antibacterial (Devi *et al*. 2010), antioxidant (Shi *et al.* 2014), and anticancer characteristics (Dwivedi *et al.* 2011). Clove oil, because of its eugenol content, has a rather higher solubility in water than other essential oils (Purwanti *et al.* 2016) and presents low toxicity.

Taking together, our findings suggest that commercial textile dye mixtures based on azo and stilbene pigments showed satisfactory results in staining and microscopy contrast compared to dyes traditionally used in plant anatomy techniques. Preliminary tests performed using double-staining technique suggest that these dyes are a promising alternative to commercially available stains for tissues. They can be used in studies that require manual cutting of fresh plant material, as well as can be successfully used for preparing material for studying plant anatomy. The mixtures investigated in this study have shown special staining efficiency to cell wall regions (consistent with their ability to stain vegetal fibers in textile materials), with a relatively greater affinity for lignified tissues. Although the MSDS from manufactures do not unequivocally identify what molecules could bind to the cell wall components and the specific binding mechanisms, a more general computational docking approximation has shown similar molecular basis of interactions for a set of representative compounds. The results of computational analyses corroborated the higher affinity of the dyes for lignin than for cellulose and are in agreement with a set of technical nuances; they provide helpful insights for future studies for the optimization of the staining intensity and selectivity. Finally, the integrated plant anatomy/computational chemistry-biochemistry approach used in this study can be didactically reproduced in interdisciplinary classes both at high school level as well as for undergraduate programs of science and engineering (in courses in the fields of biology, agronomy, forestry, and environmental engineering). Such interdisciplinary classes have been proven to be promising tools for the teaching-learning paradigm (Lima *et al.* 2009; Haynes & Leonard 2010). Hence, we expect that these results provide insights for the rational planning of low-cost and selective histological ligands and dyes for scientific and educational uses, as well as allow an environmentally sustainable alternative for using textile dyes.

Acknowledgments

The authors acknowledge the financial support provided by Fundação de Amparo à Pesquisa do Estado de Minas Gerais (FAPEMIG) and by the Coordenação de Aperfeiçoamento de Pessoal de Nível Superior (CAPES).

References

Adedayo O, Javadpour S, Taylor C, Anderson WA & Moo-Young M (2004) Decolourization and detoxification of methyl red by aerobic bacteria from a waste water treatment plant. World Journal of Microbiology and Biotechnology 20: 545-550.

Ajmal A, Majeed I, Malik RN, Iqbal M, Arif Nadeem M, Hussain I, Yousaf S, Mustafa ZG, Zafar MI & Nadeem MA (2016) Photocatalytic degradation of textile dyes on Cu2O-CuO/TiO2 anatase powders. Journal of Environmental Chemical Engineering 4: 2138-2146.

Arun PAS & Bhaskara RKV (2010) Physic chemical characterization of textile effluent and screening

for dye decolorizing bacteria. Global Journal of Biotechnology and Biochemistry 5: 80-86.

Bafana A, Devi SS & Chakrabarti T (2011) Azo dyes: past, present and the future. Environmental Reviews 19: 350-370.

Bukatsch F (1972) Bemerkungen zur Doppelfärbung Astrablau-safranin. Mikrokosmos 61: 255.

Bukowska B & Kowalska S (2003) The presence and toxicity of phenol derivatives their effect on human erythrocytes. Current Topics in Biophysics 27: 43-51.

Chowdhury S & Saha PD (2010) Sea shell powder as a new adsorbent to remove basic green 4 (malachite green) from aqueous solutions: equilibrium, kinetic and thermodynamic studies. Chemical Engineering Journal 164: 168-177.

Costa SP (2016) Uso correto de amaciantes e fixadores na estamparia têxtil com pigmentos. Available at <http://www.sintequimica.com.br/wwwroot/pdf/7/texto5.pdf>. Access on 23 September 2016.

Devi KP, Nisha SA, Sakthivel R & Pandian SK (2010) Eugenol (an essential oil of clove) acts as an antibacterial agent against *Salmonella typhi* by disrupting the cellular membrane. Journal of Ethnopharmacology 130: 107-115.

Dop P & Gautié A (1928) Manual de technique botanique. Lamarre, Paris. 594.

Dos Santos AB, Cervantes FJ & Van Lier JB (2007) Review paper on current technologies for decolourisation of textile wastewaters: perspectives for anaerobic biotechnology. Bioresource Technology 98: 2369-2385.

Douissa NB, Dridi-Dhaouadi S & Mhenni MF (2014) Study of antagonistic effect in the simultaneous removal of two textile dyes onto cellulose extracted from *Posidonia oceanica* using derivative spectrophotometric method. Journal of Water Process Engineering 2: 1-9.

Drnovsek T & Perdih A (2005) Selective staining as a tool for wood fibre characterization. Dyes Pigments 67: 197-206.

Dwivedi V, Shrivastava R, Hussain S, Ganguly C & Bharadwaj M (2011) Comparative anticancer potential of clove (*Syzygium aromaticum*) - an Indian spice - against cancer cell lines of various anatomical origin. Asian Pacific Journal of Cancer Prevention 12: 1989-1993.

Forss J & Welander U (2011) Biodegradation of azo and anthraquinone dyes in continuous systems. International Biodeterioration & Biodegradation 65: 227-237.

Gartner LP & Hiatt JL (1999) Tratado de histologia em cores. Guanabara Koogan, Rio de Janeiro. 592p.

Geneser F (2003) Histologia com bases biomoleculares. 3ª. ed. Guanabara Koogan, Rio de Janeiro. 568p.

Geng J, Tao T, Fu SJ & You W Huang W (2011) Structural investigations on four heterocyclic disperse red azo dyes having the same benzothiazole/azo/benzene skeleton. Dyes and Pigments 90: 65-70.

Gomes TC & Skaf MS (2012) Cellulose-builder: a toolkit for building crystalline structures of cellulose. Journal of Computational Chemistry 33: 1338-1346.

Goni P, Lopez P, Sanchez C, Gomez-Lus R, Becerril R & Nerin C (2009) Antimicrobial activity in the vapour phase of a combination of cinnamon and clove essential oils. Food Chemistry 116: 982-989.

Granato MA, Gaspar TM, Alves AF, de Souza AAU & Ulson SSMAG (2017) Reuse of wastewaters on dyeing of polyester fabric with encapsulated disperse dye. Environmental Technology 2: 1-10.

Hanwell M, Curtis D, Lonie D, Vandermeersch T, Zurek E & Hutchison G (2012) Avogadro: and advanced semantic chemical editor, visualization and analysis platform. J Cheminformatics 4: 1-17.

Haynes C & Leonard JB (2010) From surprise parties to mapmaking: undergraduate journeys toward interdisciplinary understanding. Journal of Higher Education 81: 645-666.

Hubbe MA, Beck KR, O'Neal WG & Sharma YC (2012) Cellulosic substrates for removal of pollutants from aqueous systems: a review. 2. Dyes. Dye biosorption: review. Bioresources 7: 2592-2687.

Irwin JJ, Sterling T, Mysinger MM & Bolstad ES (2012) ZINC: a free tool to discover chemistry for biology. Journal of Chemical Information and Modeling 52: 1757-1768.

Isenmann AF (2013) Corantes. Armin Franz Isenmann, Timóteo. 440p.

Johansen DA (1940) Plant microtechnique. McGraw-Hill, New York. 523p.

Jović-Jovičić N, Mojović Z, Darder M, Aranda P, Ruiz-Hitzky E, Banković P, Jovanović D & Milutinović-Nikolić A (2016) Smectite-chitosan-based electrodes in electrochemical detection of phenol and its derivatives. Applied Clay Science 124-125: 62-68.

Jumbo LOV, Faroni LRA, Oliveira EE, Pimentel MA & Silva GN (2014) Potential use of clove and cinnamon essential oils to control the beanweevil *Acanthoscelides obtectus* Say, in small storage units. Industrial Crops and Products 56: 27-34.

Kaiser E (1880) Verfahren zur Herstellung einer tadellosen Glycerin-Gelatine. Botanisch Zentralb 180: 25-26.

Kegley S, Conlisk E & Moses M (2010) Clove oil (Eugenol) in Marin municipal water district: herbicide risk assessment. Pesticide Research Institute, Berkeley. Pp. 1-47.

Khan S & Malik A (2018) Toxicity evaluation of textile effluents and role of native soil bacterium in biodegradation of a textile dye. Environmental Science and Pollution Research 25: 4446-4458.

Kierman JA (1990) Histological and histochemical methods: theory and practice. 3rd ed. Butterworth Heinemman, Oxford. 502p.

Kirk Jr PW (1970) Neutral red as a lipid fluorochrome. Stain Technology 45: 1-4.

Kraus JE & Arduin M (1997) Manual básico de métodos em morfologia vegetal. Editora da Universidade Federal Rural do Rio de Janeiro, Rio de Janeiro. 198p.

Kreze T, Jele S & Strnad S (2002) Correlation between structure characteristics and adsorption properties of regenerated cellulose fibre. Material Research Innovations 5: 277-283.

Kumar K, Woo AM, Siu T & Cortopassi WA (2018) Cation-π interactions in protein-ligand binding: theory and data mining reveal different roles for lysine and arginine. Chemical Science 9: 2655-2665.

Ladchumananandasivam R & Miles LWC (1994) The accessibility of cotton to anionic dyes. Journal of the Society of Dyers and Colourists 110: 300-304.

Leal CSM (2011) Solubilidade de corantes azo. Dissertação de Mestrado - Química Industrial, Universidade da Beira Interior, Covilnã. 94p.

Lima RM, Carvalho D, Sousa RM & Alves A (2009) Management of interdisciplinary approaches in engineering education: a case study. First Ibero-American Symposium on Project Approaches in Engineering Education – PAEE2009 1: 149-156.

Macedo NA (1997) Manual de técnicas em histologia vegetal. UEFS, Feira de Santana. 95p.

Mahakittikun V, Soonthornchareonnon N, Foongladda S, Boitano JJ, Wangapai T & Ninsanit P (2014) A preliminary study of the acaricidal activity of clove oil, *Eugenia caryophyllus*. Asian Pacific Journal of Allergy and Immunology 32: 46-52.

Marcucci M, Nosenzo G, Capanelli G, Ciabatti I, Corrieri D & Ciardelli G (2001) Treatment and reuse of textile effluents based on new ultrafiltration and other membrane technologies. Desalination 138: 75-82.

Martínez C, Sedano M, Munro A, López P & Pizzi A (2010) Evaluation of some synthetic oligolignols as adhesives: a molecular docking study. Journal of Adhesion Science and Technology 24: 1739-1751.

Martínez CR & Iverson BL (2012) Rethinking the term "pi-stacking". Chemical Science 3: 2191-2201.

Martínez L, Andrade R, Birgin EG & Martínez (2009) PACKMOL: a package for buliding initial configurations for molecular dynamics simulations. Journal of Computational Chemistry 30: 2157-2164.

Matthews JF, Skopec CE, Mason PE, Zuccato P, Torget RW, Sugiyama J, Himmel ME & Brady JW (2006) Computer simulation studies of microcrystalline cellulose I beta. Carbohydrate Research 341: 138-152.

Milind P & Deepa K (2011) Clove: a champion spice. International Journal of Research Ayurveda and Pharmacy 2: 47-54.

O'Brien TP & MCcully ME (1981) The study of plant structure: principles and selected methods. Termarcarphy Pty., Melburne. 45p.

Peruzzo LC (2003) Influência de agentes auxiliares na adsorção de corantes de efluentes da indústria têxtil em colunas de leito fixo. PhD Thesis. Federal University of Santa Catarina, Florianópolis. 93p.

Petridis L, Pingali SV, Urban V, Heller W, O'Neill HM, Foston M, Ragauskas A & Smith JC (2011) Self-similar multiscale structure of lignin revealed by neutron scattering and molecular dynamics simulation. Physical Review E 83: 061911: 1-4.

Purwanti N, Ichikawa S, Neves MA, Uemura K, Nakajima M & Kobayashi I (2016) b-lactoglobulin as food grade surfactant for clove oil-in-water and limonene-in-water emulsion droplets produced by microchannel emulsification. Food Hydrocolloids 60: 98-108.

Rappé AK, Casewit CJ, Colwell KS, Goddard III WA & Skiff WM (1992) UFF, a full periodic table force field for molecular mechanics and molecular dynamics simulations. Journal of the American Chemical Society 114: 10024-10035.

Rayati S & Sheybanifard Z (2016) Manganese (III) porphyrin supported onto multi-walled carbon nanotubes for heterogeneous oxidation of synthetic textile dyes and 2,6-dimethylphenol by tert-butyl hydroperoxide. Comptes Rendus Chimie 19: 371-380.

Robinson T, McMullan G, Marchant R & Nigam P (2001) Remediation of dyes in textile effluent: a critical review on current treatment technologies with a proposed alternative. Bioresource Technology 77: 247-255.

Rohde DC, Silveira SO & Vargas VRA (2006) O uso do corante urucum (*Bixa orellana* L.) na técnica de coloração histológica. Revista Brasileira de Análises Clínicas 38: 119-121.

Roy SM, Roy DR & Sahoo SK (2015) Toxicity prediction of PHDDs and phenols in the light of nucleic acid bases and DNA base pair interaction. Journal of Molecular Graphics and Modelling 62: 128-137.

Ruzin SE (1999) Plant microtechnique and microscopy. Oxford University Press, New York. 322p.

Shi C, Cui JY, Yin XF, Luo YK & Zhou ZY (2014) Grape seed and clove bud extracts as natural antioxidants in silver carp (*Hypophthalmichthys molitrix*) fillets during chilled storage: effect on lipid and protein oxidation. Food Control 40: 134-139.

Sakakibara A (1980) A structural model of softwood lignin. Wood Science and Technology 14: 89-100.

Timofei S, Kurunczi L, Schmidt W & Simon Z (2002) Steric and electrostatic effects in dye-cellulose interactions by the MTD and CoMFA approaches. SAR and QSAR Environmental Research 13: 219-226.

Vikrant K, Giri BS, Raza N, Roy K, Kim KH, Rai BN & Singh RS (2018) Recent advancements in bioremediation of dye: current status and challenges. Bioresource Technology 253: 355-367.

Villalobos MC, Cid AAP & Gonzalez AMH (2016) Removal of textile dyes and metallic ions using polyelectrolytes and macroelectrolytes containing sulfonic acid groups. Journal of Environmental Management 177: 65-73.

Walwyn V, Iglesias M, Almarales M, Acosta N, Fernández M & Cabrejas M (2004) Utilidad de técnicas histológicas para el diagnóstico de infección en piezas anatómicas. Revista Cubana de Medicina Militar 33. Available at <http://scielo.sld.cu/scielo.php?script=sci_arttext&pid=S0138-65572004000200006&lng=es&nrm=iso>.

Xing YG, Xu QL, Li XH, Che ZM & Yun J (2012) Antifungal activities of clove oil against *Rhizopus nigricans*, *Aspergillus flavus* and *Penicillium citrinum* in vitro and in wounded fruit test. Journal of Food Safety 32: 84-93.

Trott O & Olson AJ (2010) AutoDock Vina: improving the speed and accuracy of docking with a new scoring function, efficient optimization and multithreading. Journal of Computational Chemistry 31: 455-461.

Yazdanbakhsh MR, Mohammadi A & Abbasnia M (2010) Some heterocyclic azo dyes derived from thiazolyl derivatives, synthesis, substituent effects and solvatochromic studies. Spectrochimica Acta 77: 1084-1087.

Yeung EC (1998) A beginner's guide to the study of plant structure.Tested Studies for Laboratory Teaching 19: 125-141.

Yousefi H, Yahyazadeh A, Rufchahi EM & Rassa M (2013) Synthesis, spectral properties, biological activity and application of new 4-(benzyloxy) phenol derived azo dyes for polyester fiber dyeing. Journal of Molecular Liquids 180: 51-58.

Yuriev E, Holien J & Ramsland PA (2015) Improvements, trends and new ideas in molecular docking - 2012-2013 in review. Journal of Molecular Recognition 28: 581-604.

Area Editor: Dr. Diego Demarco
Received in May 24, 2018. Accepted in October 22, 2018.